Microfluidic flow-based platforms for induction and analysis of dynamic shear-mediated platelet activation—Initial validation versus the standardized hemodynamic shearing device

Annalisa Dimasi, Yana Roka-Moiia, Filippo Consolo, Marco Rasponi, Gianfranco B. Fiore, Marvin J Slepian, and Alberto Redaelli

Citation: Biomicrofluidics **12**, 042208 (2018); doi: 10.1063/1.5024500
View online: https://doi.org/10.1063/1.5024500
View Table of Contents: http://aip.scitation.org/toc/bmf/12/4
Published by the American Institute of Physics

Microfluidic flow-based platforms for induction and analysis of dynamic shear-mediated platelet activation—Initial validation versus the standardized hemodynamic shearing device

Annalisa Dimasi,[1] Yana Roka-Moiia,[2] Filippo Consolo,[1,3] Marco Rasponi,[1] Gianfranco B. Fiore,[1] Marvin J Slepian,[2,a)] and Alberto Redaelli[1,a),b)]
[1]*Department of Electronics, Information and Bioengineering, Politecnico di Milano, Via Golgi 39, 20133 Milano, Italy*
[2]*Department of Medicine and Biomedical Engineering, Sarver Heart Center, University of Arizona, 1501 N Campbell Ave, Tucson, Arizona 85724, USA*
[3]*Università Vita Salute San Raffaele, Via Olgettina 58, 20132 Milano, Italy*

(Received 1 February 2018; accepted 7 May 2018; published online 22 May 2018)

A microfluidic flow-based platform (μFP), able to stimulate platelets via exposure of shear stress patterns pertinent to cardiovascular devices and prostheses, was compared to the Hemodynamic Shearing Device (HSD)—a state-of-the-art bench-top system for exposure of platelets to defined levels and patterns of shear. Platelets were exposed to time-varying shear stress patterns in the two systems; in detail, platelets were recirculated in the μFP or stimulated in the HSD to replicate comparable exposure time. Shear-mediated platelet activation was evaluated via (i) the platelet activity state assay, allowing the measurement of platelet-mediated thrombin generation and associated prothrombotic tendencies, (ii) scanning electron microscopy to evaluate morphological changes of sheared platelets, and (iii) flow cytometry for the determination of platelet phosphatidylserine exposure as a marker of shear activation. The results revealed good matching and comparability between the two systems, with similar trends of platelet activation, formation of microaggregates, and analogous trends of activation marker exposure for both the HSD and microfluidic-stimulated samples. These findings support future translation of the microfluidic platform as a Point-of-Care facsimile system for the diagnosis of thrombotic risk in patients implanted with cardiovascular devices. *Published by AIP Publishing*. https://doi.org/10.1063/1.5024500

INTRODUCTION

Flow-based platforms are rapidly emerging as next generation approaches for the evaluation of the thrombotic risk in patients implanted with mechanical circulatory support devices (MCSDs), i.e., ventricular assist devices (VADs), mechanical heart valves, and the total artificial heart, and in patients undergoing treatment with acute blood recirculating devices (e.g., blood oxygenators). Such flow-based diagnostic platforms offer the potential for reliable evaluation of platelet responsiveness to the specific, dynamic hemodynamic environment within these devices, in contrast to conventional static non-flow diagnostic systems.

Supra-physiologic hemodynamic shear stress has been shown to act as a mechanical agonist of platelet activation, having major implications in the initiation and progression of the thrombotic process (Slepian *et al.*, 2017). In addition, recent clinical studies have firmly established an effective correlation between shear-mediated platelet activation (SMPA) and the development of thromboembolic complications in VAD patients (Valerio *et al.*, 2015; Consolo *et al.*, in

[a)]M. J. Slepian and A. Redaelli contributed equally to this work.
[b)]Author to whom correspondence should be addressed: alberto.redaelli@polimi.it. Telephone: +39 022399 4142.

press). Previous studies have characterized the platelet response to shear stress in VADs (Chiu *et al.*, 2014), mechanical heart valves (Nobili *et al.*, 2008), the total artificial heart (Marom *et al.*, 2014), and blood oxygenators (Pelosi *et al.*, 2014; Consolo *et al.*, 2016a). Moreover, we have recently shown that specific hemodynamic component elements of the shear stress pattern contribute differently to overall SMPA and that a high temporal variation of the shear stress is a major determinant of activation (Consolo *et al.*, 2017).

Despite emerging interest in flow-based platforms, their use has remained limited to laboratory and basic research activities, with translation to the clinic as effective diagnostic tools for assessing thrombogenic risk remaining to be established. The primary reason for limited translation to date stems from the fact that current bench-top flow-based systems, in the form of differing viscometer configurations (i.e., parallel-plate, Couette, or a combination of both), consist of large complex instrumentation, requiring significant volumes of the sample for a single *in vitro* test. These characteristics reduce the potential utility of these systems for use as routine diagnostic instruments. In addition, the levels of shear stress that can be replicated in these bulky laboratory devices remain limited by the pressure magnitude as "tens" of Pascals to avoid secondary flows in the fluid chamber impairing uniform stimulation of the platelet sample. Thus, shear stress conditions attainable in these systems inadequately emulate shear conditions experienced by platelets in actual clinical cardiovascular therapeutic devices.

More recently, microfluidic flow-based platforms (μFPs) have been proposed as novel approaches for evaluating shear-mediated platelet responses and associated thrombosis (Gutierrez *et al.* 2008; Hansen *et al.* 2013; Hosokawa *et al.* 2011; Li *et al.* 2014; and Li and Diamond, 2014). However, most of these systems are able to expose whole blood or platelet samples to physiologic and time-constant shear stress conditions, such as those occurring in the microcirculation. So far, the use of μFPs for the analysis of SMPA in response to highly dynamic hemodynamic conditions pertinent to cardiovascular devices has not yet been exploited.

To overcome these limitations, we developed a new computational fluid dynamic-based approach, which allows the design of specific microfluidic channels able to stimulate platelets with dynamic and highly controlled shear stress patterns of differing amplitudes (Dimasi *et al.*, 2015). Utilizing this approach, we demonstrated the feasibility of configuring μFPs to emulate realistic MCSD shear stress conditions (Consolo *et al.*, 2016b); furthermore, these microfluidic platforms were successfully utilized for testing the efficacy of differing antiplatelet agents under hyper-shear conditions (Dimasi *et al.*, 2017). The microfluidic approach, as a result of its ability to employ small sample volumes, its highly controllable working conditions, and the possibility for automation, is an attractive strategy with great potential for precision medicine. Its full translation will allow for determination of the patient-specific thrombotic risk associated with SMPA and platelet responsiveness to antiplatelet therapy readily at the bedside.

Despite the demonstrated capability of microfluidic flow-based platforms, their efficacy with regard to their defined ability to induce defined shear-mediated platelet activation has not yet been validated with respect to state-of-the-art accepted flow-based systems, as the Hemodynamic Shearing Device (HSD). The HSD is a computer-operated modified "cone and plate" and Couette viscometer designed to expose platelets to defined levels of dynamic or continuous shear stress uniformly distributed within the flow field. This well-established bench-top device allows the recreation of a wide range of shear stress conditions (either physiological or abnormal) *in vitro* and has been successfully utilized in previous studies to guide rational device design optimization and minimization of the thrombogenic potential of a range of cardiovascular devices (Sheriff *et al.*, 2014; Alemu *et al.*, 2010; Piatti *et al.*, 2015) and to develop and calibrate mathematical models of SMPA (Soares *et al.*, 2013; Sheriff *et al.*, 2013). In the present study, we hypothesized that the performance of μFPs, with regard to specific, defined shear-mediated platelet activation, will closely parallel and emulate that of the HSD, over a range of shear test conditions. As such, herein, we compared shear-mediated platelet activation, platelet shape change, and procoagulant activity, induced by exposure to dynamic shear stress conditions emulated *in vitro* in the μFP versus the HSD.

MATERIALS AND METHODS

Platelet sample preparation

30 ml of whole blood was drawn via venipuncture from healthy adult volunteers following informed consent, collected into 10% anticoagulant acid-citrate-dextrose solution, and centrifuged at 450*g* for 15 min to obtain platelet rich plasma. Platelet rich plasma was filtered through a Sepharose 2B column (Sigma-Aldrich, St. Louis, MO, USA) to obtain isolated gel-filtered platelets (GFPs). GFPs were counted using a Z1 Particle Counter (Coulter, Miami, FL, USA) and diluted to the desired final concentration (according to the specific test to be performed) in a platelet buffer consisting of Ca^{2+}-free HEPES-modified Tyrode's buffer containing 0.1% fatty-acid-free bovine serum albumin. GFPs were re-calcified with $CaCl_2$ (3 mM final concentration) 10 min prior to testing and were then exposed to dynamic shear stress patterns in μFPs or the HSD or as described below. All experiments were conducted within 6 h of phlebotomy.

Shear-mediated platelet activation in the hemodynamic shearing device

The HSD apparatus has been described in detail previously (Girdhar and Bluestein, 2008). Briefly, it consists of a programmable high-torque servo-motor controller system that drives a cone in a combined cone and plate-Couette system. The HSD fluid chamber configuration allows exposure of the sample to uniform shear stress. The device can be programmed to generate highly dynamic patterns of shear stress in a step-like manner (with a resolution up to 3 ms).

To induce SMPA in the HSD, human GFPs were subjected to devised dynamic shear stress conditions replicating specific features characteristics of MCSDs. In detail, simulated shear stress patterns are characterized by repetitive peaks of shear stress with a fixed peak value (5 Pa) and differing peak durations and time intervals between consecutive peaks. These time-varying dynamic shear patterns, termed as Dyn1 and Dyn2, were selected to be properly replicated by the HSD, i.e., avoiding secondary flows in the fluid chamber impairing uniform stimulation of the platelet sample. The dynamic shear stress curve is shown in Fig. 1; Dyn1 and Dyn2 shear stress pattern characteristics are specified in Table I.

Dyn1 and Dyn2 were programmed in the HSD. For each curve, 3.5 ml of re-calcified GFPs (100 000 cells/μl) was placed in the HSD fluid chamber. The system was first run for 10 s at 0.1 Pa to allow leveling out the GFPs in the shearing chamber, at which point the specific shearing program (either Dyn1 or Dyn2) was initiated. For the time point sample collections (TP, TPs 1–4), the system was programmed to slow down to 0.1 Pa for 30 s to allow collection of 200 μl of sheared GFPs, performed by manually withdrawing the sample with a 1 ml plastic tuberculin syringe connected to a lateral access port of the fluid chamber via polyethylene tubing (1.0 mm internal diameter and 5 cm length). Upon collection, samples were immediately processed for platelet activation analyses as described below. For each blood donor, consecutive tests were conducted for Dyn1 and Dyn2 shear conditions. Between consecutive tests, the HSD chamber and the collection system were extensively flushed with HEPES-modified buffer, while

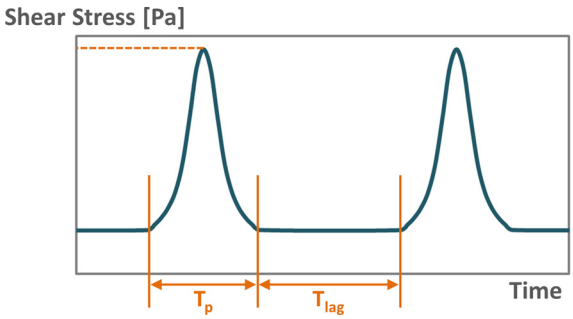

FIG. 1. Curve of the dynamic shear stress pattern utilized in the study. Repetitive triangular-shaped peaks characterized by a fixed peak of shear stress (5 Pa) but with differing peak duration (T_p) and time between consecutive peaks (T_{lag}).

TABLE I. Characteristics of dynamic shear stress pattern conditions. The baseline (τ_{base}), peak shear stress (τ_{peak}), peak duration (T_p), time between consecutive peaks (T_{lag}), and shear exposure time (time points, TP 1–4) are reported.

	Shear stress curve characteristics				Time points (TPs)			
	τ_{base} (Pa)	τ_{peak} (Pa)	T_p (ms)	T_{lag} (ms)	TP 1	TP 2	TP 3	TP 4
Dyn1	1	5	40	90	1′	3′	6′	9′
Dyn2	1	5	160	360	1′	3′	6′	9′

between different donors, the system was flushed with 0.5% Sodium dodecyl sulphate in 50 mM NaOH, followed by extensive flushing with the HSD platelet-contacting surfaces using Sigmacote® (Sigma Aldrich, USA), followed by air drying.

Microfluidic channel design and platform fabrication

The microfluidic platform was designed according to the approach described by our group previously (Dimasi *et al.*, 2015). Briefly, the geometry of each model is designed according to preliminary analytical formulae and then optimized through the Computational Fluid Dynamics analyses; multiphase computational fluid dynamic analyses are run in which the fluid dynamic in the microfluidic channel is simulated while calculating the trajectories of thousands of virtually injected platelets.

The dynamic shear stress curves along platelet trajectories in the microchannel are then exported and analyzed. From all the shear stress curves, a representative curve is extracted: for this aim, shear stress curves are summarized in a scalar index, i.e., the stress accumulation, calculated as the linear integral of the shear stress over time, and the curve closest to the median of the distribution of the stress accumulation value is selected as the representative shear stress curve of the channel.

Finally, a semi-automatic iterative algorithm allows us to optimize channel geometrical parameters (widths and lengths of the shear stress-generating features) based on the discrepancy between descriptive parameters of the shear stress waveforms along platelet trajectories in the microfluidic channels and the reference shear stress waveform to be replicated.

To replicate Dyn1 and Dyn2, two specific channel geometrical configurations were identified as shown in Fig. 2. Microchannel dimensions were chosen as a compromise between standard photo-lithography manufacturing capabilities, while guaranteeing the validity of continuum flow hypothesis used in the designing process (Dimasi *et al.*, 2015), and the need for limiting

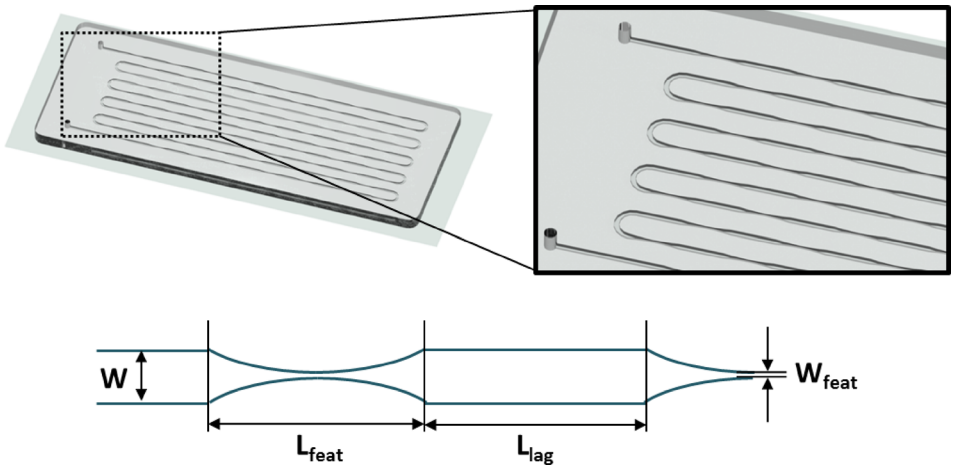

FIG. 2. A microfluidic platform for dynamic shear stress conditions. Top panel: 3D Computer Aided Design (CAD) model of a μFP sample, with a zoomed view on the channel features. Bottom panel: schematic drawing of the μFP channel design where geometrical parameters are reported.

TABLE II. Geometrical characteristics of the two different microfluidic channels replicating Dyn1 and Dyn2 shear stress curves and the corresponding flow rates. The channel height (h), width (W), and length (L) are reported together with the parameters referring to geometrical characteristics of the channel features generating the shear stress peaks: the width and length of the feature (W_{feat} and L_{feat}), the length of the straight portion of the channel between consecutive features (L_{lag}), and the total number of features on the same channel (N_{feat}). In both cases, a flow rate value Q equal to 15 μl/min was used.

	h (μm)	W (μm)	W_{feat} (μm)	L_{feat} (mm)	L_{lag} (mm)	N_{feat}	Q (μl/min)
Dyn1	50	200	44	2	1.75	288	15
Dyn2	50	200	44	8	7.00	72	15

the flow rates and hence the pressures in the microchip. The channels are characterized by subsequent cross-section narrowings, whose dimensions are reported in Table II: W_{feat} and L_{feat} and L_{lag} refer to the width and length of the narrowing feature and the length of the straight portion of the channel between consecutive features, respectively. N_{feat} indicates the number of feature repetitions on a single channel. The latter was set to guarantee estimated pressure drops across the platforms below 2 atm to avoid fluid leakage during the test performance.

Micropatterned silicon wafers were fabricated via standard photolithography using a negative photoresist SU-8 2050 (Microchem Corp, USA) in a cleanroom facility. Fabrication of the microfluidic platforms was then obtained by replica molding of polydimethylsiloxane and subsequent sealing on 35 mm × 50 mm cover glasses through plasma bonding. A 3D CAD model of a representative μFP is shown in Fig. 2.

Microfluidic platform testing

Recirculation of the GFP sample in the μFP was implemented to allow exposure time to shear longer than TP 1 and to match time points of platelet analysis as used in HSD experiments. For this aim, two synchronized syringe pumps operating in the reciprocating mode were employed, via which GFPs were alternatively pumped back and forth through the μFP in a closed hydraulic system. In detail, two syringe pumps (AL2000, World Precision Instrument, UK) equipped with 250 μl precision glass syringes (Hamilton Gastight 1725 TLL syringes) were connected to 508 μm internal diameter Tygon® tubes 25 cm long through 23 G disposable blunt needles. Tubes were then connected to the access ports of the μFP through two stainless steel couplers (23G, 1 cm long). The setup for μFP recirculation experiments is shown in Fig. 3.

After passivating the μFP tubing with 3% w/v bovine serum albumin in phosphate buffered saline (PBS) for 1 h at room temperature, and subsequently washing with PBS, each tube was filled with 45 μl of re-calcified GFP sample (100 000 cell/μl) by withdrawal from a 0.65 ml

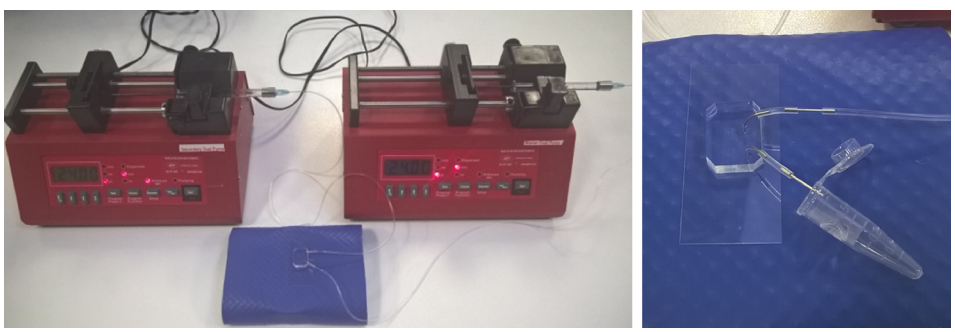

FIG. 3. Setup of synchronized syringe pumps for reciprocating pumping of GFPs in the μFP (left panel). The picture of the microfluidic platform during the sample collection that followed GFP recirculation (right panel).

Eppendorf tube at the predefined flow rate (see Table II) via the syringe pumps. One tube was connected to the μFP, and filling was started by pumping the GFP sample at the same flow rate. A sample of 15 μl at the outlet of the μFP was first discarded, and the remaining 30 μl was collected as the TP 1 sample for Platelet Activation State (PAS) assay and scanning electron microscopy (SEM) analysis (as described in the next two sections). The second tube was then connected to the free port of the platform to close the system, and the reciprocating pumping was started: 40 μl of GFP in the second tube was alternatively pumped back and forth through the μFP until the desired shearing time (TPs 2, 3, or 4) was achieved. At this point, the system was opened, and 30 μL of sheared sample was collected in a 0.65 ml Eppendorf tube (Fig. 3, right panel) and tested.

For the PAS assay, 3 consecutive tests were performed on the same platform to obtain TP 1 and TP 2 in the first run and TP 3 and TP 4 in two further runs. Between consecutive runs, the system was extensively flushed with PBS. Two different platforms replicating Dyn1 and Dyn2, respectively, were tested with the same blood donor.

Scanning electron microscopy

Scanning electron microscopy (SEM) was performed to visualize early platelet morphological changes, occurring as a result of dynamic shear exposure to Dyn1 and Dyn2 in HSD and μFPs. The serial SEM images were acquired on samples exposed to shear at 2 different time points (TP 1 and TP 4 as defined in Table I). Following shear exposure, 30 μl aliquots of GFP (100 000 cells/μl) was deposited on glass coverslips (13 mm diameter). Samples were immediately fixed by adding 30 μl of 2% v/v glutaraldehyde in HEPES-modified platelet buffer. After 30 min incubation at room temperature, coverslips were washed through successive dilutions of glutaraldehyde in ddH_2O. Finally, successive dilutions of ddH_2O in ethanol (up to 100% ethanol) were used to dehydrate the samples. Coverslips were mounted on metal stubs using double-sided adhesive carbon tape. After gold-coating treatment performed using an Anatech Hummer 6.6 (Anatech, USA) sputter system, SEM image acquisitions were performed on an FEI Inspec-S SEM (FEI Company, USA). As an unstimulated control, intact GFP samples were also imaged. SEM imaging was performed on 2 different donors.

Platelet activity state assay

To characterize the dynamics of SMPA over the shear exposure time, a chromogenic platelet activity state (PAS) assay measuring thrombin generation on the surface of shear-stimulated platelets was utilized (Jesty and Bluestein, 1999). Specifically, GFP samples collected from the μFP and the HSD at differing time points (TP 1–4) were assessed. 25 μl aliquot of sheared GFP (20 000 cells/μl) was incubated for 10 min at 37 °C in the presence of acetylated prothrombin, $CaCl_2$, and factor Xa. During the incubation, acetylated prothrombin is activated into acetylated thrombin by factor Xa, and the enzymatic reaction rate directly depends on the prothrombotic activity of platelets (i.e., their activation level induced by shear exposure). Unlike the native enzyme, acetylated thrombin possesses amidolytic activity on the peptide substrate and is incapable of activating platelets in a positive feedback manner, allowing stoichiometric correlation of thrombin generation rate to the actual level of SMPA (Jesty and Bluestein, 1999). To quantify thrombin generation, a VersaMax^{TM} ELISA Microplate Reader (Molecular Devices LLC, CA, USA) was used. Kinetic measurements of absorbance changes were conducted in the presence of a chromogenic substrate for thrombin, Chromozym TH (Roche, Switzerland). The rate of absorbance change obtained for each sheared GFP sample was normalized against the corresponding values of sonicated GFP. As sonication induces maximum prothrombinase activity, PAS values are reported as a percentage of sonicated SMPA, with 100% activation established from measured sonicated samples. GFPs were sonicated at 75 W (40 kHz) for 10 s using an ultrasonic device (SLPE Branson, USA). PAS experiments were conducted on 6 different donors.

Flow cytometry detection of platelet phosphatidylserine exposure

To detect phosphatidylserine exposure induced by shear stress, an annexin V binding assay was performed. The principle of the assay is based on the high affinity binding of the protein annexin V labeled with fluorescent dye to phospholipid phosphatidylserine exposed on the platelet surface as a result of activation or apoptosis. For flow cytometry analyses, GFPs were used at a concentration of 100 000 cells/μl. Following shear exposure (at TP 4), 30 μl of collected GFP was incubated with 5 μl Fluorescein Isothiocyanate (FITC)-conjugated annexin V (Molecular Probes, USA) in 70 μl of binding buffer consisting of 10 mM HEPES, 140 mM NaCl, and 2.5 mM $CaCl_2$ at pH 7.4. After 30 min incubation at room temperature in the dark, samples were fixed by adding 300 μl of 4% v/v paraformaldehyde in PBS. After 20 min, samples were centrifuged at 5000 rpm for 5 min, the supernatant was removed, and the platelet pellet was re-suspended in 500 μl of 50 mM phosphate buffer free of Ca^{2+} and Mg^{2+}. This step was performed twice, and the sample was transferred in 12×75 mm polystyrene Falcon tubes. Flow cytometric analysis was performed on a FACScan flow cytometer (BD Biosciences, San Jose, CA, USA) equipped with an air-cooled 15 mW argon ion laser tuned to 488 nm. The emission fluorescence of FITC-conjugated Annexin V was detected and recorded through a 530/30 bandpass filter in the FL1 channel. List mode data files consisting of 10 000 events gated on forward scatter (FSC) vs side scatter (SSC) were acquired. Raw data exported as fcs files were subsequently analyzed using Matlab® 2015b (Mathworks, USA). Appropriate electronic compensation was adjusted by acquiring unstimulated GFPs stained with the fluorophore and unstained GFPs as a control for autofluorescence. A positive control was also tested consisting of GFPs stimulated in the HSD system at a constant shear stress of 7 Pa for 10 min. Flow cytometry analyses were performed on two different donors.

Statistical analyses

Statistical analyses of assay results were performed with GraphPad Prism 7.2 (GraphPad Software, Inc., CA, USA). Normal distribution of data was first tested with the Shapiro-Wilk normality test. One-way Analysis of Variance (ANOVA) was used when normality hypothesis was satisfied for all the groups being tested. Alternatively, non-parametric Kruskal–Wallis one-way ANOVA was performed. For multiple comparisons, the Bonferroni post-hoc test was used to test significant differences between groups. The statistical significance was assumed for p-values < 0.05.

RESULTS AND DISCUSSION

The current study focused on the comparability of platelet activation induced via shear exposure within microfluidic flow-based platforms (μFPs), which generate shear stress via traverse through defined complex geometry channels, as compared with activation induced via shear exposure in the established standard, programmable HSD modified cone and Couette system. Two simulated dynamic shear stress patterns (Dyn1 and Dyn2) characterized by repetitive peaks of shear stress with a fixed peak value (5 Pa) and differing peak durations and time intervals between consecutive peaks were employed. These time-varying dynamic shear patterns were selected to be properly replicated by the HSD, i.e., avoiding secondary flows in the fluid chamber impairing uniform stimulation of the platelet sample. To evaluate platelet activation and function alterations, the followings were done: (i) changes in the platelet morphology, as an early marker of SMPA, were examined via SEM; (ii) platelet procoagulant activity driven by shear exposure was determined as the rate of thrombin generation measured via the PAS assay; and (iii) flow cytometry detection of annexin V binding was conducted to reveal phosphatidylserine exposure as a result of platelet membrane reorganization in response to shear stress.

Platelet morphology alterations induced by dynamic shear stress

Platelet samples exposed to Dyn1 and Dyn2 shear patterns via the μFP or the HSD were acquired at TP 1 and TP 4, corresponding to 1 and 8 min of shear exposure time, respectively. At TP 1 of shear exposure, morphological characteristics of SMPA were observed in both μFP-

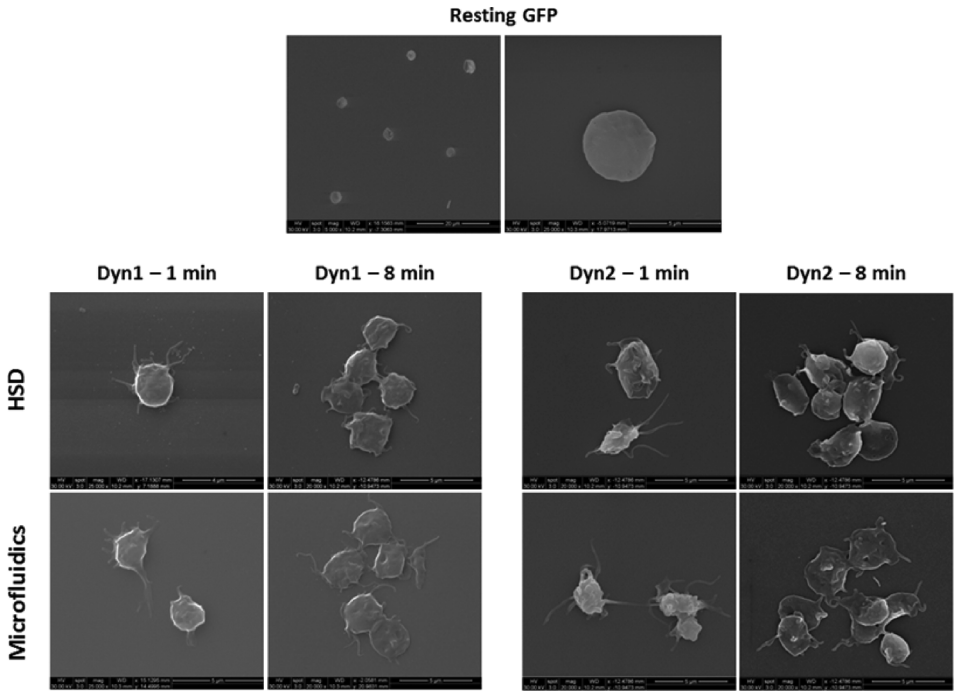

FIG. 4. Morphologic changes of human platelets subjected to dynamic shear stress patterns Dyn1 and Dyn2 in the microfluidic platforms ("Microfluidics") and the hemodynamic shearing device ("HSD") as compared with intact platelets ("Resting GFP"). SEM images were acquired at TP 1 (1 min) and TP 4 (8 min) of shear exposure.

and HSD-sheared platelet samples (Fig. 4, "Dyn1—1 min"). Specifically, platelet contraction and filopodia extrusion were prominently observed in the shear-stimulated platelets, as compared to the preservation of a discoid morphology and homogeneous membrane configuration in non-stimulated platelet controls (Fig. 4, "Resting GFP"). No relevant differences between μFP- and HSD-shear stimulated samples in terms of platelet morphology alterations were found. This agreement obtained between microfluidic platforms and the HSD provides supportive evidence that controlled shear stress conditions can be effectively generated in the μFP by properly modulating the channel geometry design. Interestingly, after longer exposure time to shear (TP 4) in the μFP and the HSD, microaggregates of platelets were observed following stimulation with either Dyn1 or Dyn2 shear patterns.

Platelet procoagulant activity driven by dynamic shear exposure in μFP and HSD

The extent of platelet activation followed by exposure to dynamic shear stress was evaluated using the PAS assay, as a functional approach measuring the rate of thrombin activation by factor Xa on the platelet surface after stimulation. In Fig. 5, the results of the PAS assay

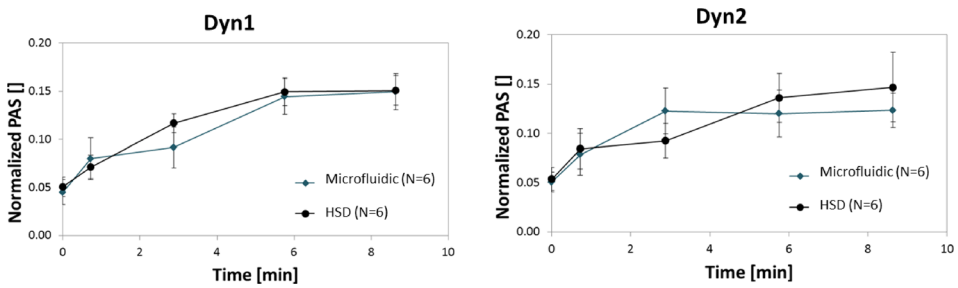

FIG. 5. Platelet procoagulant activity induced by exposure to dynamic shear stress patterns Dyn1 and Dyn2 in the microfluidic platforms ("Microfluidic") and the hemodynamic shearing device ("HSD"). The results are reported as mean ± standard deviation.

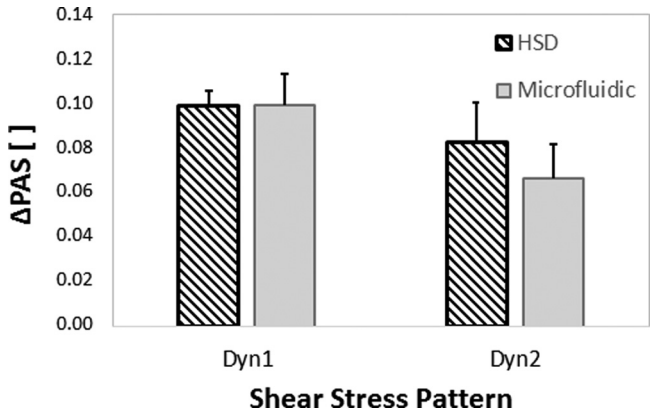

FIG. 6. The increase in platelet activity state levels after exposure to dynamic shear stress patterns Dyn1 and Dyn2 (ΔPAS, TP 4 and TP 0) via the microfluidic platform ("Microfluidic") and the hemodynamic shearing device ("HSD"). The results are reported as mean ± standard deviation (n = 6).

performed on GFP sheared via the μFP and the HSD are reported for Dyn1 and Dyn2 at differing time points (from 0 to 9 min). For both dynamic shear patterns, a time-dependent increase in SMPA was observed. For longer exposure times (TP 3 to TP 4), a smaller increase in SMPA was noted. This is in agreement with previous studies on SMPA in which similar trends and PAS levels were obtained by exposing platelets in the HSD to dynamic shear stress conditions comparable to those considered in the present study (Sheriff *et al.*, 2013).

In Fig. 6, the PAS difference between TP 4 and non-stimulated control is reported according to Sheriff *et al.*, 2013. Comparable PAS values were obtained in the μFP and the HSD for both Dyn1 and Dyn2 shear patterns (Dyn1: $p = 0.96$; Dyn2: $p = 0.31$). Although not statistically significant, the Dyn2 condition was associated with a lower increase in platelet activation with respect to control, both in the HSD and μFP. This result is again in agreement with a previous study in which lower activation was observed from dynamic and periodic shear stress patterns characterized by longer time periods of the dynamic waveform (Sheriff *et al.*, 2013). Indeed, Dyn2 is characterized by a time period of 520 ms, compared to 130 ms of Dyn1.

In Fig. 7, the correlation curve between PAS data obtained in the HSD and in the μFP is shown for both Dyn1 and Dyn2 (left panel). The Bland-Altman plot obtained from the same data is reported in Fig 7 (right panel). A good correlation between microfluidic- and HSD-stimulated platelets was observed ($R^2 = 0.62$). From the Bland-Altman plot, no systematic or proportional difference phenomenon was found, suggesting that similar levels and trends of platelet activation can be achieved by properly designing the μFP channel geometry.

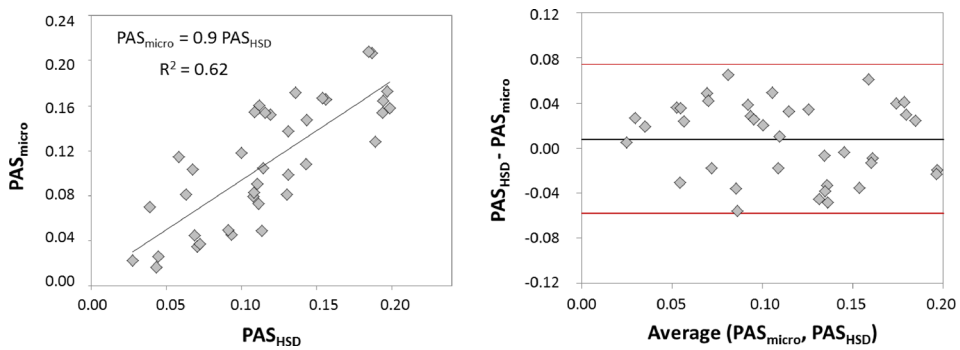

FIG. 7. Correlation between PAS results obtained in the microfluidic platforms and in the HSD (left panel) and Bland-Altman plot (right panel).

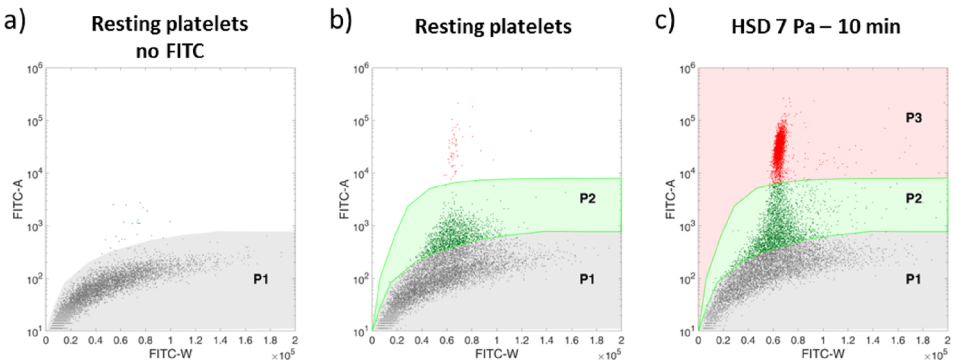

FIG. 8. Fluorescence pulse area (FITC-A) versus width (FITC-W) in control platelet samples: (a) unstained non-stimulated platelets (autofluorescence control), (b) non-stimulated platelets (negative control), and (c) platelets exposed to 7 Pa continuous shear stress in the HSD for 10 min (positive control).

Platelet phosphatidylserine exposure resulting from exposure to dynamic shear

Flow cytometry was performed to examine platelet membrane eversion and aminophospholipid exposure following dynamic shear stimulation in the μFP as compared with the HSD. Platelets presenting phosphatidylserine on their surface were identified via an annexin V binding assay. Different platelet populations were distinguished based on two output fluorescence parameters: the fluorescence pulse area (FITC-A) and the fluorescence pulse width (FITC-W). The gate setup and annexin V-positive platelet population distribution are reported in Fig. 8; intact platelets and high-shear stimulated platelets are shown as negative and positive controls, respectively. The unstained control [Fig. 8(a)] was employed to define the gate for platelet autofluorescence (P1 region) and to identify platelets not binding annexin V on their surface. Consequently, gates P2 and P3 represent two platelet populations (outside of the P1 region) binding different levels of annexin V: the P3 region—clearly distinguishable in the positive control—identifies the population of platelets characterized by a very high fluorescence pulse area, while region P2 identifies platelet population with lower annexin V binding and was defined as the intermediate region between P1 and P3.

Representative populations at the FITC-A vs FITC-W plane for the Dyn1 and Dyn2 samples at TP 4 are reported in Fig. 9 for both the HSD- and μFP-stimulated platelets. Overall, all sheared samples showed a greater density P2 region as compared to the negative stained control [Fig. 8(b), "Resting platelets"], indicating an increase in platelet phosphatidylserine exposure after shear stimulation. A slight increase in platelet density in the P3 region, as compared to negative stained control, was indeed observed in HSD-stimulated samples (both Dyn1 and Dyn2) but not evident in μFP-stimulated samples.

The heterogeneity of identified platelet populations (P1, P2, and P3) for Dyn1 and Dyn2 samples is shown at histogram of FITC-A distribution (Fig. 10). Slightly higher qualitative prevalence of platelets in the P2 and P3 regions was observed in HSD-stimulated samples. A quantitative comparison is provided in Table III, where the values of population prevalence (expressed as percentage over the total events acquired) and the mean values of FITC-A in P1, P2, and P3 are reported. Also, the same values obtained for the negative stained control are shown (resting platelets).

A decrease in the platelet number in the P1 region was found for all sheared samples with respect to controls, with a corresponding increase in the platelet number in the P2 region, indicative of increased platelet binding of annexin V. The last observation is aligned with PAS results, showing an increase in thrombin generation of sheared samples with respect to non-stimulated platelets (Fig. 5). Indeed, aminophospholipid exposure on the platelet outer membrane provides a surface for the assembly of the prothrombinase complex, which in turn leads to thrombin formation. Overall, a low prevalence of platelets in the P3 region was found for all conditions tested. In the Dyn1 condition, a larger difference was obtained between HSD- and

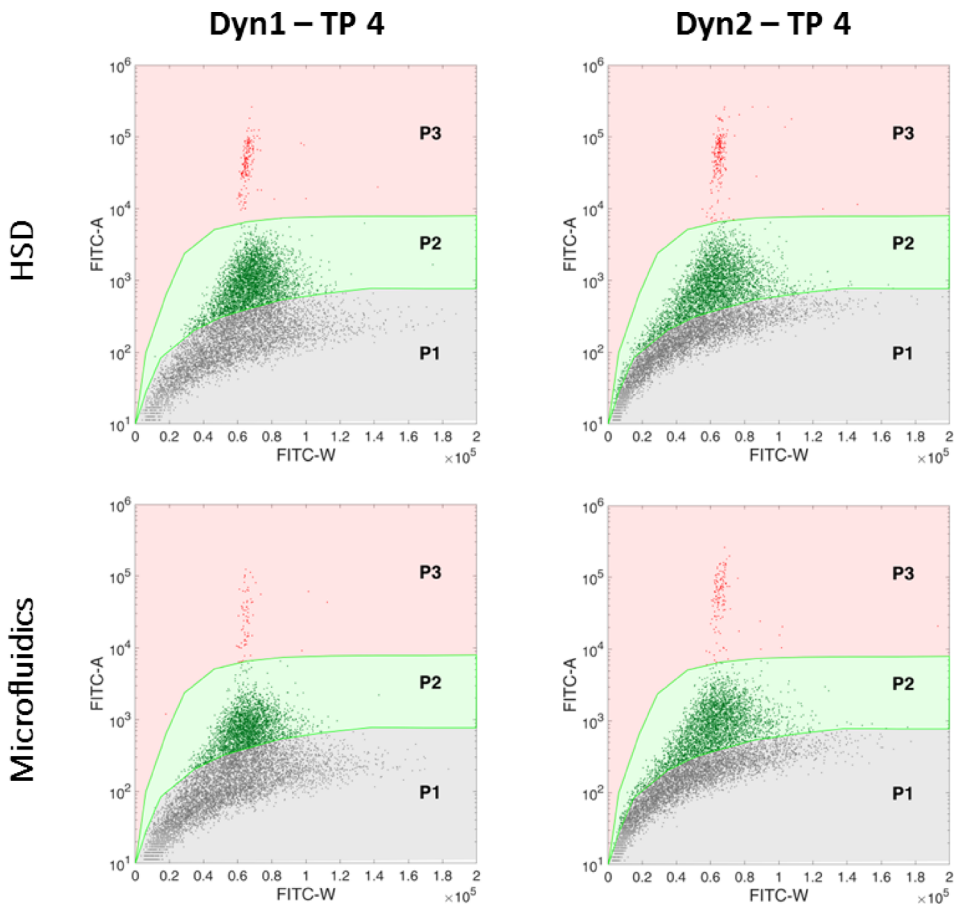

FIG. 9. Phosphatidylserine exposure on platelet surfaces following stimulation (TP 4) with dynamic shear patterns Dyn1 (a) and Dyn2 (b) applied in the HSD (top) and microfluidic platforms (bottom).

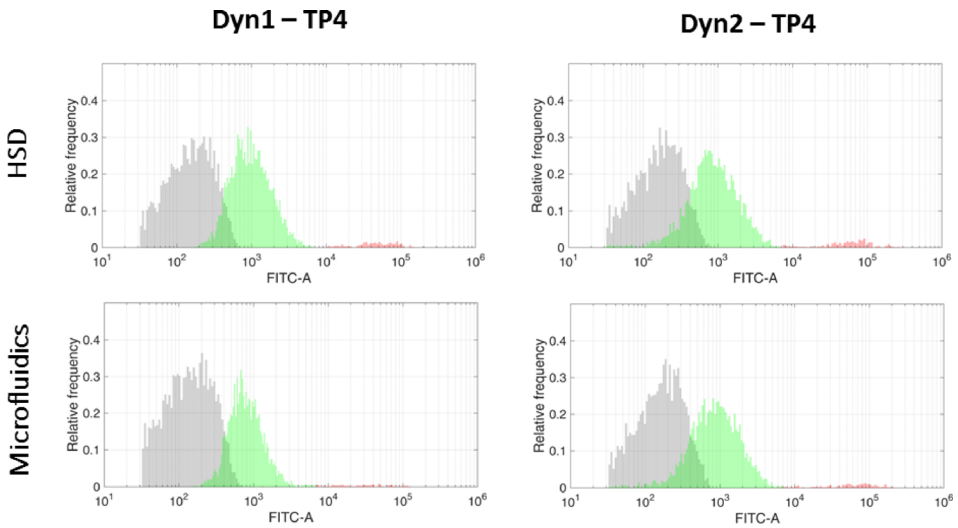

FIG. 10. Histogram distributions of FITC-A of the three separate populations (P1 grey, P2 green, and P3 red) for Dyn1 (a) and Dyn2 (b) shear stress conditions at TP 4 from the HSD (top) and the microfluidic platforms (bottom). The values of FITC-A in the P3 population were reported only when a prevalence greater than 1% was found.

TABLE III. Platelet population heterogeneity (P1, P2, and P3) for the shear stress conditions tested (Dyn1 and Dyn2) in the HSD system and the microfluidic platforms.

	Population prevalence (%)			Mean FITC-A (AU)		
	P_1	P_2	P_3	P_1	P_2	P_3
Resting platelets	80	19	1	145	700	…
Micro–Dyn1	66	33	1	161	900	…
HSD–Dyn1	54	44	2	176	1000	52 000
Micro–Dyn2	57	42	2	185	1000	67 000
HSD–Dyn2	54	44	2	186	1000	67 000

μFP-sheared samples. A better matching was found between HSD and microfluidics for the Dyn2 condition.

Interestingly, in terms of uniformity of FITC-A distribution, no relevant differences were obtained in the microfluidic and HSD systems. This result is of particular interest in the present study as it shows that despite the fact that the microfluidic shearing platform is intrinsically characterized by a larger variability of shear stress conditions (due to fluid paths characterized by different shear stresses and exposure times in the same channel), this intrinsic variability is not reflected in a larger heterogeneity of pro-coagulant marker expression among the population of platelets when compared to the HSD. The latter indeed is purposely designed to generate a uniform shear stress field in the sample chamber.

Flow cytometry analyses thus provided a further insight into the evaluation of the microfluidic shearing system, showing that similar distributions of platelet response in terms of peak stress exposure following controlled shear stress conditions in microfluidic and HSD systems could be obtained.

CONCLUSION

In the present study, we assessed microfluidic flow-based platforms, designed via a computational fluid dynamic-based approach to emulate shear stress patterns and components of mechanical circulatory support devices, as to their efficacy of inducing shear-mediated platelet activation in comparison to that achieved with the accepted and established laboratory-standard approach of the hemodynamic shearing device system. Specifically, the dynamics of platelet activation over a range of differing shear exposure times was evaluated via (a) the PAS assay—a chromogenic assay of platelet thrombin generation, (b) SEM imaging of morphologic alterations of sheared platelets, and (c) flow cytometry analysis—to evaluate platelet exposure of activation markers (Annexin V). In this study, we found that comparable trends of PAS values were obtained with the microfluidic platform in comparison to the HSD. Furthermore, we demonstrated that microfluidic flow-based platforms induced comparable formation of platelet microaggregates, as compared with those formed with the HSD, particularly for longer shear exposure times. These SEM results morphologically confirm the functional activation data demonstrated via the PAS assay result. Flow cytometry similarly revealed an analogous trend of exposure of activation markers with microfluidic flow-based platforms as was generated with identical shear exposure in the HSD. All in all, these results provide functional biochemical (PAS assay), morphologic (SEM), and marker (Annexin V) data, confirming the similarity and efficacy of microfluidic flow-based platforms (μFP) as effective, reliable, practical small footprint surrogates of defined shear pattern platelet activation in comparison to the HSD.

Value and advantages of microfluidic flow-based platforms (μFPs)

Microfluidic flow-based platforms (μFPs) extend the armamentarium of methodologies available for fluid and mechanobiologic studies of platelet activation from several perspectives. Microfluidic platforms require minimal volumes of blood for analysis. Typically, 1–2 ml of

blood is all that is needed to generate the few microliters of platelets—presently with conventional upstream processing to separate platelets from whole blood—then load, and run platelets through the (μFP) shear channels. In the future, with incorporation of an integrated upstream platelet separation capability, blood requirements may conceivably be further reduced to a minimal requirement of a finger prick—i.e., with $<$100 microliters, for such a system. Present μFPs, as well as envisioned integrated system μFPs, would extend utility and analysis to small animal research in which overall blood volumes are minimal and obtaining samples is more difficult. Microfluidic flow-based platforms (μFPs) also offer the advantage of reduced consumption of reagents. Buffers and antibodies, affording an overall reduction in the cost of analysis.

Microfluidics offers the potential for automated processing, which could be readily integrated with a μFP system for pre-processing and post-processing steps—i.e., for isolation of platelets from whole blood and for assay incorporation (PAS), allowing quantization of platelet activation. In the literature, indeed, several examples of microfluidic approaches have been described to separate blood components (e.g., hydrophoresis: Hou *et al.*, 2015) and to measure platelet activation (e.g., aggregometry: Schimmer *et al.*, 2013), which support our concept of an eventual integrated system being developed based on the herein described μFPs.

From a flow perspective, microfluidic flow-based platforms (μFP) allow attainment of very high shear stress levels under laminar flow regimes, thus replicating hyper-shear values and dynamics occurring in prosthetic cardiac devices. Additionally, their characteristic high surface-to-volume ratio implies extremely controlled and precise handling of fluids and compounds, i.e., for highly repeatable processes. In comparison, the HSD is a bulky system, requiring large volumes of blood and significant reagent volumes, and has been limited in its use as to the level of shear stress generated. Furthermore, the large volume requirement has made small animal investigation difficult if not prohibitive, e.g., for mice, and is not amenable to clinical translation as either a laboratory or point-of-care instrument.

Study limitations

The two dynamic shear stress conditions tested (Dyn 1 and Dyn 2) were selected in order to guarantee effective uniform stimulation of platelets within the HSD. As they were found to result in similar levels of platelet activation, this observation may raise some concerns, as we were not able to evaluate the sensitivity of the microfluidic flow-based platform compared to the HSD. From this perspective, future studies should be further expanded to the analysis of shear stress conditions with differing characteristics in terms of shear stress patterns inducing eventually differing platelet activation levels.

Future implications and translation

Nonetheless, this is the first study in which a microfluidic flow-based platform was employed to replicate dynamic shear stress conditions, whose hemodynamic characteristics were selected to simulate device-like hemodynamic conditions and associated shear stress (the repetitive exposure to the peak of shear stress resembles cyclic platelet recirculation through the device). As such, this study is a positive step for the future translation and development of a Point-of-Care microfluidic platform for bed-side assessment of patient-specific prothrombotic risk.

ACKNOWLEDGMENTS

This work was funded by Fondazione Cariplo and Regione Lombardia [Grant No. 2016-0901] and Fondazione Cariplo [Grant No. 2015-1044] and received support from the University of Arizona Center for Accelerated Biomedical Innovation (ACABI) and Tech Launch Arizona [Grant No. UA 15-035].

The authors would like to acknowledge UACC/ARL Cytometry Core Facility (Arizona Cancer Center, Tucson, USA) for providing flow cytometry analyses, which were funded by the Cancer Center Support Grant (CCSG-CA 023074). The W.M. Keck Center for Surface and Interface Imaging (University of Arizona, Tucson, USA) and PoliFab (Politecnico di Milano, Italy) are also

acknowledged for providing facility for SEM image acquisitions and the micro- and nanofabrication facility, respectively.

Alemu, Y., Girdhar, G., Xenos, M., Sheriff, J., Jesty, J., Einav, S., and Bluestein, D., "Design optimization of a mechanical heart valve for reducing valve thrombogenicity—A case study with ATS valve," ASAIO J. **56**, 389–396 (2010).

Chiu, W.-C., Girdhar, G., Xenos, M., Alemu, Y., Soares, J. S., Einav, S. *et al*., "Thromboresistance comparison of the heartmate ii ventricular assist device with the device thrombogenicity emulation-optimized HeartAssist 5 VAD," J. Biomech. Eng. **136**, 021014 (2014).

Consolo, F., Dimasi, A., Rasponi, M., Valerio, L., Pappalardo, F., Bluestein, D., Slepian, M. J., Fiore, G. B., and Redaelli, A., "Microfluidic approaches for the assessment of blood cell trauma: A focus on thrombotic risk in mechanical circulatory support devices," Int. J. Artif. Organs **39**, 184–193 (2016b).

Consolo, F., Sferrazza, G., Motolone, G., Contri, R., Valerio, L., Lembo, R., Pozzi, L., Della Valle, P., De Bonis, M., Zangrillo, A., Fiore, G. B., Redaelli, A., Slepian, M. J., and Pappalardo, F., "Platelet activation is a preoperative risk factor for the development of thromboembolic complications in patients with continuous-flow left ventricular assist device," Eur. J. Heart Failure **20**, 792–800 (2018).

Consolo, F., Sheriff, J., Gorla, S., Magri, N., Bluestein, D., Pappalardo, F., Slepian, M. J., Fiore, G. B., and Redaelli, A., "High frequency components of hemodynamic shear stress profiles are a major determinant of shear-mediated platelet activation in therapeutic blood recirculating devices," Sci. Rep. **7**, 4994 (2017).

Consolo, F., Valerio, L., Brizzola, S., Rota, P., Marazzato, G., Vincoli, V. *et al*., "On the use of the platelet activity state assay for the in vitro quantification of platelet activation in blood recirculating devices for extracorporeal circulation," Artif. Organs **40**(10), 971–980 (2016a).

Dimasi, A., Rasponi, M., Consolo, F., Fiore, G. B., Bluestein, D., Slepian, M. J., and Redaelli, A., "Microfludic platforms for the evaluation of anti-platelet agent efficacy under hyper-shear conditions associated with ventricular assist devices," Med. Eng. Phys. **48**, 31–38 (2017).

Dimasi, A., Rasponi, M., Sheriff, J., Chiu, W. C., Bluestein, D., Tran, P. L., Slepian, M. J., and Redaelli, A., "Microfluidic emulation of mechanical circulatory support device shear-mediated platelet activation," Biomed. Microdevices **17**, 117 (2015).

Girdhar, G. and Bluestein, D., "Biological effects of dynamic shear stress in cardiovascular pathologies and devices," Expert Rev. Med. Devices **5**(2), 167–181 (2008).

Gutierrez, E., Petrich, B. G., Shattil, S. J., Ginsberg, M. H., Groisman, A., and Kasirer-Friede, A., "Microfluidic devices for studies of shear-dependent platelet adhesion," Lab Chip **8**, 1486–1495 (2008).

Hansen, R. R., Wufsus, A. R., Barton, S. T., Onasoga, A. A., Johnson-Paben, R. M., and Neeves, K. B., "High content evaluation of shear dependent platelet function in a microfluidic flow assay," Ann. Biomed. Eng. **41**, 250–262 (2013).

Hosokawa, K., Ohnishi, T., Kondo, T., Fukasawa, M., Koide, T., Maruyama, I. *et al*., "A novel automated microchip flow-chamber system to quantitatively evaluate thrombus formation and antithrombotic agents under blood flow conditions," J. Thromb. Haemostasis. **9**, 2029–2037 (2011).

Hou, H. W., Bhattacharyya, R. P., Hung, D. T., and Han, J., "Direct detection and drug-resistance profiling of bacteremias using inertial microfluidics," Lab Chip **15**, 2297–2307 (2015).

Jesty, J. and Bluestein, D., "Acetylated prothrombin as a substrate in the measurement of the procoagulant activity of platelets," Anal. Biochem. **272**, 64–70 (1999).

Li, M., Hotaling, N. A., Ku, D. N., and Forest, C. R., "Microfluidic thrombosis under multiple shear rates and antiplatelet therapy doses," PLoS One **9**, e82493 (2014).

Li, R. and Diamond, S. L., "Detection of platelet sensitivity to inhibitors of COX-1, P2Y(1), and P2Y(1)(2) using a whole blood microfluidic flow assay," Thromb. Res. **133**(2), 203–210 (2014).

Marom, G., Chiu, W. C., Crosby, J. R., DeCook, K. J., Prabhakar, S., Horner, M., Slepian, M. J., and Bluestein, D., "Numerical model of full-cardiac cycle hemodynamics in a total artificial heart and the effect of its size on platelet activation," J. Cardiovasc. Transl. Res. **7**, 788–796 (2014).

Nobili, M., Sheriff, J., Morbiducci, U., Redaelli, A., and Bluestein, D., "Platelet activation due to hemodynamic shear stresses: Damage accumulation model and comparison to in vitro measurements," ASAIO J. **54**, 64–72 (2008).

Pelosi, A., Sheriff, J., Stevanella, M., Fiore, G. B., Bluestein, D., and Redaelli, A., "Computational evaluation of the thrombogenic potential of a hollow-fiber oxygenator with integrated heat exchanger during extracorporeal circulation," Biomech. Model. Mechanobiol. **13**, 349–361 (2014).

Piatti, F., Sturla, F., Marom, G., Sheriff, J., Claiborne, T. E., Slepian, M. J. *et al*., "Hemodynamic and thrombogenic analysis of a trileaflet polymeric valve using a fluid-structure interaction approach," J. Biomech. **48**, 3650–3658 (2015).

Sheriff, J., Girdhar, G., Chiu, W. C., Jesty, J., Slepian, M. J., and Bluestein, D., "Comparative efficacy of in vitro and in vivo metabolized aspirin in the DeBakey ventricular assist device," J. Thromb. Thrombolysis **37**, 499–506 (2014).

Sheriff, J., Soares, J. S., Xenos, M., Jesty, J., Slepian, M. J., and Bluestein, D., "Evaluation of shear-induced platelet activation models under constant and dynamic shear stress loading conditions relevant to devices," Ann. Biomed. Eng. **41**(6), 1279–1296 (2013).

Schimmer, C., Hamouda, K., Sommer, S. P., Özkur, M., Hain, J., and Leyh, R., "The predictive value of multiple electrode platelet aggregometry (multiplate) in adult cardiac surgery," Thorac. Cardiovasc. Surg. **61**, 733–743 (2013).

Slepian, M. J., Sheriff, J., Hutchinson, M., Tran, P., Bajaj, N., Garcia, J. G. N., Scott Saavedra, S., and Bluestein, D., "Shear-mediated platelet activation in the free flow: Perspectives on the emerging spectrum of cell mechanobiological mechanisms mediating cardiovascular implant thrombosis," J. Biomech. **50**, 20–25 (2017).

Soares, J. S., Sheriff, J., and Bluestein, D., "A novel mathematical model of activation and sensitization of platelets subjected to dynamic stress histories," Biomech. Model. Mechanobiol. **12**, 1127–1141 (2013).

Valerio, L., Consolo, F., Bluestein, D., Tran, P., Slepian, M., Redaelli, A., and Pappalardo, F., "Shear-mediated platelet activation in patients implanted with continuous flow LVADs: A preliminary study utilizing the platelet activity state (PAS) assay," in *Proceedings of the Annual International Conference of the IEEE Engineering in Medicine and Biology Society, EMBS* (2015), pp. 1255–12583.